JP1.2 THE KA`Ū STORM: IMAGING PRECIPITABLE WATER USING GPS

James Foster*, Michael Bevis, Steven Businger and Yi-Leng Chen
University of Hawaii, Honolulu, HI

1. INTRODUCTION

The Ka`ū (pronounced Ka-oo) Storm was an extreme rain event that impacted the south and east sides of the Big Island of Hawai`i during the 1st and 2nd of November, 2000. Maximum hourly rain-rates were over 100 mm/hr (~4 in/hr) and the total rainfall from the storm reached nearly 1000 mm at one location, with a 24-hour accumulation that fell just short of setting a state record. Stream gauge records show that this was the most intense, widespread rain event in 20 years, and at several sites the maximum stream-flow from this storm established records. The extensive flash floods that resulted are estimated to have caused $70M property damage and the impacts on roads and other infrastructure persisted for weeks afterwards. Intriguingly, several days after this huge water-load was deposited on the island GPS sites recorded the first documented instance of an aseismic slip event on Kīlauea Volcano (Cervelli et al. 2002). This suggests that a shallow fault may have been activated by the increased pore-pressure due to this excess of water, and raises the question of whether landslides might also be a delayed but significant hazard from extreme rainfall events in this area.

The maximum rainfall was recorded by the rain gauge at Kapāpala Ranch on the south slope of Mauna Loa (Figure 1). This gauge recorded 989 mm (>39 inches) of rain over 36 hours and heavy rainfall was recorded over most of the southern and eastern portions of the Island. Previous studies have investigated this pattern of heavy rain event on the south-facing slopes of Hawai`i (Kodama and Barnes, 1997, Schroeder, 1978) and have interpreted the large temporal scales of the heavy precipitation and the quasi-stationary nature as the effect of orographic lifting which anchors the storm to the mountainous terrain when the winds are blowing onshore.

* *Corresponding author address*: James Foster, POST 602, 1680 East West Road, 1680 East West Road, Honolulu, HI 96822; e-mail jfoster@soest.hawaii.edu

The formation of the deep convection required for heavy rain is controlled by the depth of the moist layer depth and the interaction of the surface winds with the islands' complex topography. The NCEP Global Spectral Model, which, with about 1-degree grid spacing, does not include topography for the Hawaiian Islands, failed to predict any of the subsequent rainfall. The more detailed Regional Spectral Model (10-km grid) run operationally by NWS/U.H. Dept. Meteorology (Wang et al. 1998) which incorporates coarse topography was able to predict some rainfall, but it was both grossly underestimated, and mislocated. Only with the inclusion of detailed topography in a 3-km grid Mesoscale Spectral Model (Zhang et al. 2000; http://www.soest.hawaii.edu/~rsm), run after the event, was a more realistic model of the actual rainfall generated although even then the predicted rainfall was only 50-60% of the actual measured values. This highlights the potential contribution that an all-weather GPS system could make in providing rapid and accurate precipitable water (PW) estimates, particularly in concert with satellite data, for which GPS could provide point PW calibrations (Motell et al., 2000).

A network of GPS receivers (Fig. 1) covers much of Kīlauea and the summit of Mauna Loa, allowing us to calculate frequent, accurate estimates for the precipitable water over much of the area most affected by the storm. With sites at elevations from sea level to over 4000 m at the summit, and with an average spacing of less than 10 km this network provides us with a unique opportunity to examine the details of the precipitable water distribution as the storm passed over the southeastern section of the island.

2. DATA AND METHODOLOGY

The Big Island GPS network consists of 7 receivers run by the Pacific GPS Facility, 15 more operated by the Hawaiian Volcano Observatory (HVO-USGS) and Stanford University, and one final receiver (MKEA) available from the International GPS Service (IGS). The rain gauge data is compiled from the National Weather Service Hydronet network with

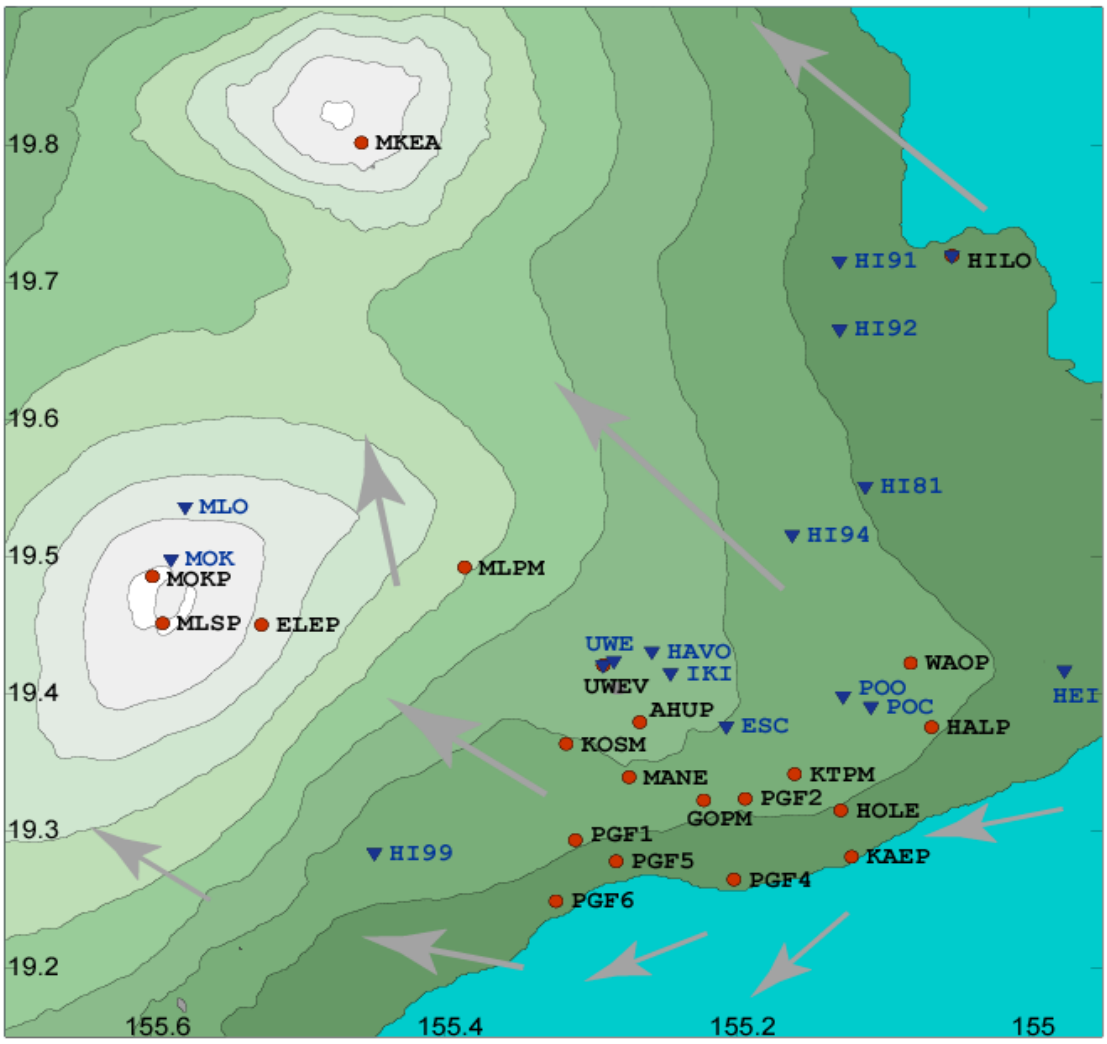

FIG. 1. Location map of the Big Island GPS and rain gauge networks. Red circles with black labels are GPS sites, blue labels with blue triangles are rain gauges. Elevation is shaded with 500 m contours. Regional surface wind field for the storm is interpreted with light gray arrows.

additional data from the National Park Service AIRS program and HVO's tiltmeter network.

Although the spatial coverage of the GPS receivers is very good, only the PGF (PGF1, PGF2, PGF4, PGF5, PGF6 and HILO) and JPL (MKEA) receivers (see Figure 1) have collocated meteorological instruments to provide the surface pressure and temperature measurements needed to directly estimate the PW. Hawaii is famous for its microclimates (Juvik 1978) due to the orographic effects of the huge volcanoes. Rainfall in particular varies dramatically over very short horizontal distances (Giambelluca 1986) but all surface meteorological parameters are affected and have complex local variations. The extreme relief across the GPS network compounds this problem, making it very difficult to accurately extrapolate pressure and temperature fields any distance from the measurement points.

The solution that we adopted was to include data from the NCEP Reanalysis. Pressure, temperature and dew point were interpolated from the reanalysis to each GPS site. The coarse (2.5 degree) grid for the reanalysis is naturally unable to reproduce the details of the island's meteorological patterns, however the mean values for each site predicted from this grid were typically very close to the mean measured values; not surprising, as to a first approximation we are simply located in the middle of the ocean. A correction field for the

NCEP-predicted data was calculated by modeling the misfits between the observed data and the NCEP-predicted data using linear spatial gradients and offsets. As the magnitudes of the misfits from the measured data are small, the exponential form of the pressure can be ignored and all the fields treated as behaving linearly, simplifying the procedure. These final predicted data, interpolated to the GPS atmospheric knot epochs match the measured data to ~. 25 mbar and ~1.5 deg-C rms while preventing the extrapolated fields from tending to unrealistic values away from observation points. The accuracies typically required for pressure and temperature data for use in GPS meteorology are 0.3 mbar (Saastamoinen, 1971) and 3 deg-C (Emardson and Derks, 2000) indicating that the extrapolated fields are sufficiently accurate for this study.

GPS data from the all of the Big Island sites running during the storm were processed using a sliding window technique (Fang et al. 1999). In this technique a moving time window is used to select data for processing. Although this technique can be used with no sequential window overlap in order to minimize the processing time, allowing a significant overlap for each window has the advantage of producing several estimates for each time epoch. These multiple estimates allow for an internal check on the accuracy of the solution, and allow us to find a robust average for each epoch. This also avoids a problem that plagues the more traditional batch processing where the switch from one 24-hour orbit solution to the next causes a "boundary effect" at the poorly constrained window edges where sequential solutions appear to be offset from each other at their common epoch. The processing package GAMIT (King and Bock 2000) was used along with precise orbits solutions from the Scripps Orbit and Permanent Array Center (SOPAC) to generate solutions for the 10 days covering the storm. The processing window was 8 hours wide and stepped forward in hourly increments, with atmospheric estimates made every 15 minutes using a piecewise constant function.

Internal consistency checks of the GPS atmospheric solutions suggest that the final ZND estimates are accurate to better than 10 mm. External checks are more problematic: the NWS radiosonde launches in Hilo failed during the storm (incidentally illustrating one of the advantages GPS has over many of the traditional meteorological instruments) and although there is a second Hawaiian NWS radiosonde launch site in Līhu`e, Kaua`i, the GPS receiver at the site was, unfortunately, not operational during this period. As no local independent verification of the GPS estimates was possible for the storm event we have to rely for our error estimates and on previous experience. Motell et al. (2001) found that the rms difference between PW from the Līhu`e radiosonde and the GPS site was ~1.7 mm. As a significant component of that difference must be due to errors in the radiosonde PW retrieval, and studies of GPS PW accuracy elsewhere indicate similar or better accuracy (for example, Tregoning et al. 1998; Fang et al. 1998) we conclude that the absolute accuracy for those sites with surface meteorological data is ~1.5 mm of PW while for the other sites the combined errors in the GPS solutions and surface meteorological field extrapolations translate to an accuracy of ~2 mm of PW.

3. TEMPORAL STRUCTURE OF PW

Figure 2 shows a montage of precipitable water time-series from 5 GPS sites. From PGF6, located near sea level on the south shore of Kīlauea the sites step upslope, roughly northwards to MLSP on the summit of Mauna Loa. The bottom panel shows the rain gauge record for Kapāpala ranch, the location of the highest recorded rainfall for the storm, and located slightly to the west of this profile.

The five traces show the same general pattern for the storm, imaging a strong initial drying event followed by a rapid rise in PW with the high maintained through the night of 1st to the 2nd of November. In detail, however, there are several interesting differences. The preliminary drying event, and the subsequent rapid rise in PW during morning of the 1st occurs later at the higher elevations: the trough at MLPM reaches a minimum a little after the lower three sites and persists longer. At MLSP, well above the inversion layer, on the summit of Mauna Loa, the PW is actually still rising slightly when the lower sites reach their minimums (time "a"), before showing a brief, small trough while the others have already begun to climb strongly. The drying event is probably related to subsidence in front of the approaching storm, perhaps enhanced by the diurnal katabatic flow as the island cools during the night (Feng and Chen 2001)

Notably, while the lower sites continue to see an increase in PW until mid-morning of the 2nd of November, MLPM starts to decrease earlier, and MLSP reached its peak values at

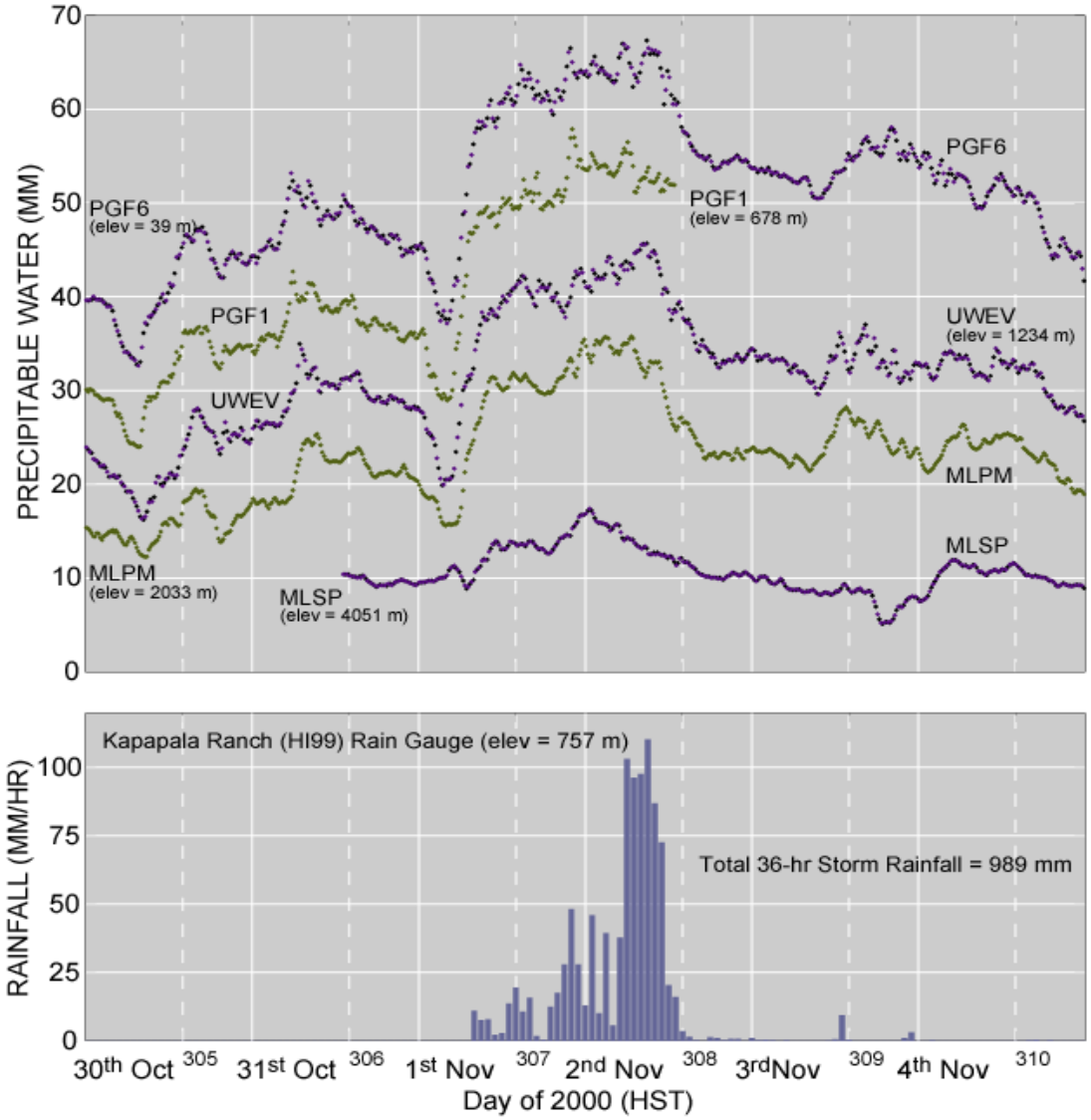

FIG. 2. Time series for 5 selected GPS sites. Lower panel shows the rainfall record from Kapapala Ranch rain gauge (HI99) location of the highest accumulated rainfall for the storm.

about midnight and declines throughout the day. The rain data reflect the same pattern with rainfall at Kapāpala Ranch peaking mid-morning, and rainfall at Hilo and Moku`āweoweo peaking at midnight. This suggests that there were two main rainfall episodes, the first primarily affecting Hilo and the north-eastern slopes of Mauna Loa and the second more locally focused on the south-eastern slopes at the western edge of the GPS network (the Ka`ū district).

The details of the sub-peaks that are superimposed on the broad PW high are subtly different between all the sites, probably reflecting the small-scale variability inherent in the atmosphere. Although some of the peaks are clearly correlated between sites, for others correlations are less obvious, illustrating the small-scale structure of PW field.

The PGF1 time-series is a dramatic testament to the flash floods that accompanied the peak rainfall of this event. PGF1 is located several meters above a storm stream channel. The abrupt end of its time-series, shortly after the peak rainfall recorded at Kapāpala Ranch, records when the floods become so intense that they inundated the surrounding area and washed the GPS receiver box down the hill,

ripping out the antenna cable and short-circuiting the electronics. The receiver was recovered near the lip of a ~1000 ft cliff, was repaired and the data were recovered. PGF6 located on the coastal plain below PGF1 and near the edge of the alluvial fan deposited by such flood-events narrowly avoided a similar fate.

4. PW AND RAINFALL

There are 4 GPS sites in the network that have rain gauges located within a few kilometers. As the GPS antennas and rain gauges are close to each other we can reasonably assume that they recorded the same events at the same time, giving us the opportunity to examine in detail the relationship between the PW and rainfall. These 4 pairs constitute an east-west profile from near sea level at Hilo to ~4050 m at the top of Mauna Loa. The total rainfall for these gauges for the 36 hours of the event ranges from 100 mm (~4 inches) on the summit of Mauna Loa to 785 mm (~30 inches) in Hilo, with the peak rainfall occurring during the night of Nov 1st and early morning of Nov 2nd local time (HST=UTC-10). The first significant rainfall occurs during the rapid PW rise during the early morning of 1st Nov. as the moist air first reaches the island. The rain typically begins as the PW reaches between 2 and 3 geometric standard deviations (GSD) above the median and increases in intensity with increasing PW.

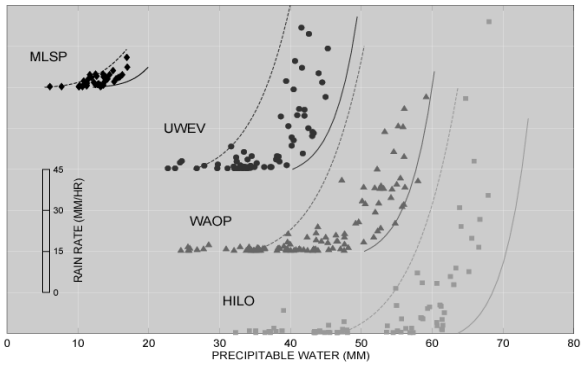

FIG. 3. Rainfall vs precipitable water for four sites with GPS and rain gauges located in close proximity. Lines are based on an expontial function of the number of geometric standard deviations of precipitable water and represent bounds on heavy rainfall. The dashed lines indicatesthe earliest possible onsets of heavy rainfall, while the solid lines represent the levels at which heavy rainfall will definitely have commenced.

Examining the relationship between PW and rainfall (Fig. 3) shows that although there is broad scatter for low-rainfall events, for each site significant rainfall starts at PW levels above 1.75 GSD above normal, with rates non-linearly dependent on PW above this point. Once the PW reaches 3 GSD all sites show rainfall. Note

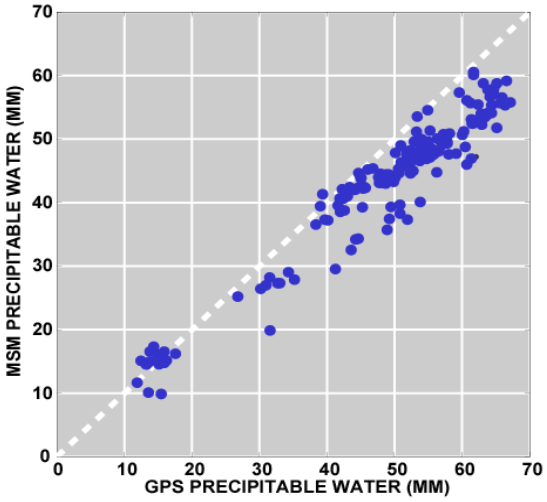

FIG. 4. Comparison of MSM predicted precipitable water with GPS-derived estimates. Dashed white lines indicates the 1:1 ratio. MSM is clearly persistently underestimating precipitable water for moist copnditions.

that Hilo records heavy rainfall at lower PW GSD levels than the other sites. This may be partly due to a sensitivity to the exact value of the geometric standard deviation when mapping from measured PW to the normalized PW, or may simply reflect the inadequacy of this method to fully represent the physical processes.

5. GPS AND THE MSM

Comparing the MSM predicted PW with the GPS estimated PW (Fig. 4) shows that the MSM is clearly underestimating PW for most of the range, and particularly for higher values. The effect this has on the rainfall predictions is illustrated in Figure 5 where the MSM misfits for the precipitable water and the rainfall at the same four GPS/rain gauge site pairs used to generate the GPS rainfall algorithm above are shown. Although the data show broad scatter and one extreme outlier, the linear correlation between the underestimate of PW and the underestimate of rainfall is clear. Encouragingly the best-fit line passes very close to the origin, indicating that where the PW is well modeled the predicted rainfall also matches the observations, suggesting that there is no inherent bias in the MSM predictions.

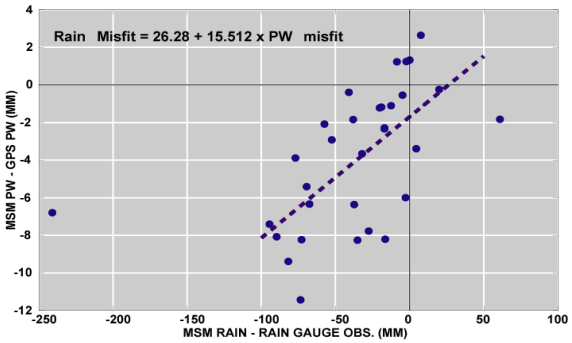

FIG. 5. Plot showing the misfit in MSM predicted precipitable water against the misfit in predicted rainfall. Best L1-norm fit line is shown. Underestimated rainfall is clearly correlated with underestimated precipitable water suggesting that rainfall predictions might be improved by better constraining the precipitable water field.

6. CONCLUSIONS

We use a GPS network over Kīlauea and Mauna Loa volcanoes to image the precipitable water field of the Ka`ū Storm, as it passed over this portion of the island. The subsidence ahead of the system, and rapid increase in PW as the storm impacts the island are clearly visible in the time series. The timing of the main PW peaks across the network along with the rain gauge records suggests that there were two main rain events, while short period spikes illustrate the small-scale variability of the PW field.

Comparing the GPS derived PW with the rainfall and PW predicted by the MSM predictions we conclude that the shortfall in the MSM rainfall predictions is largely due to its underestimate of PW. Although incorporating GPS PW data into the MSM is likely to be of limited benefit in terms of weather forecasting as it can only provide information on the PW over the islands and not for the critical upstream zone, the fact the PW was underestimated by the MSM for virtually every epoch at every location suggests that the GPS PW could at least help provide better initialization values, leading to some improvement in its performance, particularly in extreme weather.

A more valuable role for GPS in weather forecasting for island locations however would be to provide absolute PW calibrations for satellite maps of the regional PW field. This would combine the accuracy and continuous time coverage of GPS with the broad spatial coverage, but low absolute accuracy PW available from satellites.

References

Cervelli, P., P. Segall, K. Johnson, M. Lisowski, and A. Miklius, Sudden aseismic fault slip on the south flank of Kīlauea Volcano, *Nature*, *415* (6875), 1014-1018, 2002.

Emardson, T.R., and H.J.P. Derks, On the relationship between the wet delay and the integrated precipitable water vapour in the European atmosphere., *Meteorol. Appl.*, *7*, 61-68, 2000.

Fang, P., M. Bevis, Y. Bock, S. Gutman, and D. Wolfe, GPS meteorology: Reducing systematic errors in geodetic estimates for zenith delay, *Geophys. Res. Lett.*, *25*, 3583-3586, 1998.

Fang, P., Y. Bock, and M.v. Domselaar, Hourly updated GPS orbit prediction using sliding window approach, *International Symposium on GPS*, 1999.

Feng, J., and Y.-L. Chen, Numerical simulations of airflow and cloud distributions over the windward side of the Island of Hawaii. Part II: Nocturnal flow regime, *Mon. Wea. Rev.*, *129*, 1135-1147, 2001.

Giambelluca, T.W., M.A. Nullet, and T.A. Schroeder, Hawaii Rainfall Atlas, pp. 267, Hawaii Division of Water and Land Development, Department of Land and Natural Resources, Honolulu, 1986.

Juvik, S.P., and J.O. Juvik, Atlas of Hawaii, University of Hawai`i Press, Honolulu, 1998.

King, R.W., and Y. Bock, Documentation for the GAMIT GPS Analysis Software version 10.03, Massachusets Institute of Technology, Cambridge, 2000.

Kodama, K., and G.M. Barnes, Heavy Rain Events over the South-Facing Slopes of Hawaii: Attendant Conditions, *Wea. Forecasting*, *12* (2), 347-367, 1997.

Motell, C., J. Porter, J. Foster, M. Bevis, and S. Businger, Comparison of precipitable water over Hawaii using AVHRR-based split-window techniques, GPS and radiosondes, *Int. J. Remote Sens.*, *23* (No. 11), 2335-2339, 2002.

Saastamoinen, J., *Atmospheric correction for the troposphere and stratosphere in radio ranging of satellites*, AGU, 1972.

Schroeder, T.A., Mesoscale Structure of Hawaiian Rainstorms, pp. 69pp, Water Resources Research Center, Honolulu, 1978.

Tregoning, P., R. Boers, D. O'Brien, and M. Hendy, Accuracy of absolute precipitable water vapor estimates from GPS

observations, *J. Geophys. Res.*, *103*, 28,701-28,710, 1998.

Wang, J.-J., H.-M.H. Juang, K. Kodama, S. Businger, Y.-L. Chen, and J. Partain, Application of the NCEP Regional Spectral Model to Improve Mesoscale Weather Forecasts in Hawaii, *Wea. Forecasting*, *13* (3), 560-575, 1998.

Zhang, Y.-X., Y.-L. Chen, H.-M.H. Juang, S.-Y. Hong, K. Kodama, and R. Farrell, Validation and sensitivity tests of the mesoscale spectral model simulations over the Hawaiian islands, *2nd Regional Spectral Model Workshop*, *MHPCC, Maui, Hawaii*, 2000.